Available online at www.sciencedirect.com
SCIENCE DIRECT
Trans. Nonferrous Met. Soc. China 16(2006) 357−362
Transactions of Nonferrous Metals Society of China
www.csu.edu.cn/ysxb/

Microstructure and property of sub-micro WC-10 %Co particulate reinforced Cu matrix composites prepared by selective laser sintering

GU Dong-dong(顾冬冬)[1], SHEN Yi-fu(沈以赴)[1], DAI Peng(代 鹏)[1], YANG Ming-chuan(杨明川)[2]

1. College of Materials Science and Technology, Nanjing University of Aeronautics and Astronautics, Nanjing 210016, China;
2. Shenyang National Laboratory for Materials Science, Institute of Metal Research, Chinese Academy of Sciences, Shenyang 110016, China

Received 19 September 2005; accepted 29 November 2005

Abstract: The WC-10%Co particulate reinforced Cu matrix composite material with a WC-Co∶Cu mass ratio of 20∶80 was successfully fabricated by selective laser sintering(SLS) process. The following optimal processing parameters were used: laser power of 700 W, scan speed of 0.06 m/s, scan line spacing of 0.15 mm, and powder layer thickness of 0.3 mm. The microstructure, composition, and phase of the laser processed material were investigated by scanning electron microscopy(SEM), X-ray diffraction(XRD), and energy dispersive X-ray(EDX) spectroscopy. The results show that the bonding mechanism of this process is liquid phase sintering. The Cu and Co act as the binder phase, while the WC acts as the reinforcing phase. The non-equilibrium effects induced by laser melting, such as high degrees of undercooling and high solidification rate, result in the formation of a metastable phase $CoC_{0.25}$. The WC reinforcing particulates typically have three kinds of morphology. They are agglomerated and undissolved, incompletely separated and partially dissolved, separated and dissolved, which indicates that particle rearrangement acts as the dominant sintering mechanism for the larger WC, while dissolution-precipitation prevails for the smaller WC particles. Microhardness tester was used to determine the Vickers hardness across the cross-section of the laser sintered sample, with the average value being $HV_{0.1}$268.5. However, the hardness varied considerably, which might be attributed to the WC segregation and the high solidification rate experienced by the molten pool.

Key words: selective laser sintering; metal matrix composites; Cu matrix composite; WC-Co; Cu; microstructure; microhardness

1 Introduction

Selective laser sintering(SLS) is one of a few rapid prototyping(RP) techniques, which enables fabrication of three-dimensional(3D) parts with arbitrary shapes directly from metal powder with no or minimal post-processing[1−3]. In this method, an object is created by selectively sintering or/and melting thin layers of powder with a scanning laser beam according to CAD data[4,5]. The main advantages associated with this technique are high design flexibility, excellent process capabilities, and time- and cost-saving features[6−8]. Currently, metallic SLS process has been commercially available to produce high performance engineering parts, e.g. functional prototypes and low-volume tooling for injection molding and die casting[9−12].

It is known that WC-Co hard metals are widely used for cutting and drilling tools and for wear resistance applications because of the combination of high strength, high hardness, and high toughness[13−16], while copper is also extensively used because of its excellent electrical and thermal conductivities, outstanding resistance to corrosion, and fatigue resistance[6,10]. The preparation of WC-Co particulate reinforced Cu matrix composite materials is expected to combine their superior mechanical and thermal properties. Generally, WC-Co reinforced metal matrix composites(MMCs) are produced by conventional casting and powder metallurgy methods. These techniques are productive and can achieve fully dense structures, but they need expensive and dedicated tools. Therefore, it is not suitable for small

Foundation item: Project(10276017) supported by the Joint Fund of National Natural Science Foundation of China and China Academy of Engineering Physics; Project(04H52061) supported by the Aeronautical Science Foundation of China; Project(S0403-061) supported by the Scientific Research Innovations Foundation of Nanjing University of Aeronautics and Astronautics
Corresponding author: SHEN Yi-fu; Tel: + 86-25-85687494; E-mail: yifushen@nuaa.edu.cn

volume production and complex shapes[17]. In fact, due to the flexibility in material and shape, SLS has the possibility for creating some special kinds of MMCs that cannot be created by other methods.

In this study, WC-Co particulate reinforced Cu matrix composite material is prepared via direct SLS. The microstructure, composition and microhardness of the composites are investigated, with a total aim to assess the feasibility of creating hard metals particulate reinforced MMCs by SLS process.

2 Experimental

2.1 Powder preparation

Electrolytic 99% purity Cu powder with spherical shape and mean particle size of 15 μm and WC-10%Co composite powder with mean equivalent spherical diameter of 0.8 μm were used in this experiment. The WC-Co composite powder was synthesized using a novel 'spray drying and fixed bed' technique[18], which involved spray drying a precursor solution containing AMT-Co$(NO_3)_2$, followed by roasting, ball milling, reduction, and carbonization.

The two components were mixed according to Cu∶WC-Co mass ratio of 80∶20. Powder dispersion was performed in a cylindrical vessel with a vacuum-pumping system at a rotation speed of 150 r/min for 60 min, with ball to powder mass ratio of 5∶1. The scanning electron microscopy(SEM) image of the mixed powder system is shown in Fig.1.

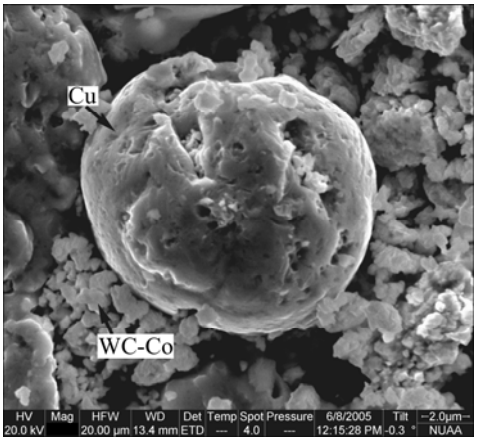

Fig.1 SEM image of starting powder mixture

2.2 Laser processing

The SLS apparatus in this experiment mainly consisted of a CW, 2000 W, CO_2 Gaussian laser beam and related optics, an automatic powder delivery mechanism, and a process controlling computer. When a test specimen was to be built, the process computer sliced its CAD model into a stack of thin slices of 0.3 mm thickness. The data preparation step was followed by the laser sintering process. Firstly, a steel substrate was placed on the building platform in the processing cylinder. Then, a uniform thin layer of powder was deposited on the substrate by the roller. Subsequently, a laser beam scanned the powder bed to form a layer-wise profile according to the CAD data. The similar process was repeated until the part was completed.

The following optimal laser processing parameters were used: spot size of 0.30 mm, laser power of 700 W, scan speed of 0.06 m/s, and scan line spacing of 0.15 mm. The entire laser processing was performed at room temperature without atmosphere control. The real-time laser sintering process is shown in Fig.2(a). It can be seen that the powder was smoothly sintered without any obvious splash. The rectangular specimen with dimensions of 50 mm×10 mm×6 mm was successfully fabricated, showing very little dimensional deformation (Fig.2(b)).

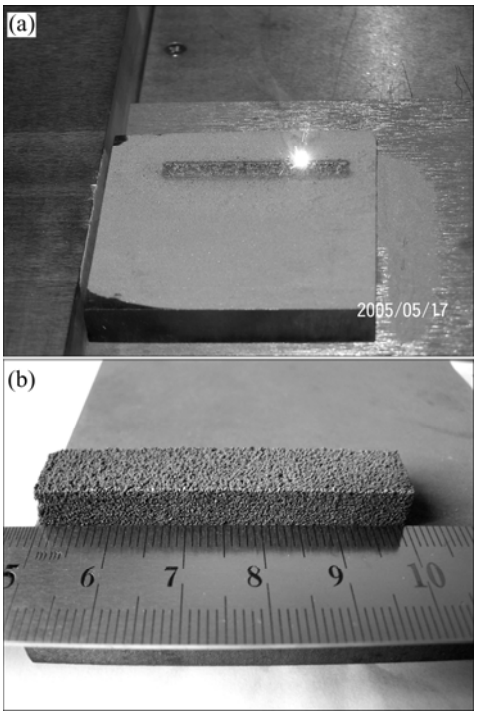

Fig.2 Photographs of laser sintering process(a) and laser sintered sample(b)

2.3 Characterization

Samples for metallographic examination were prepared according to the standard procedures and etched with a mixture of $FeCl_3$ (10 g), HCl (20 mL) and distilled water (100 mL) for 2 min. Phase identification of the raw powder mixture and the laser sintered sample was performed using a BRUKER D8 ADVANCE X-ray diffraction(XRD) analyzer. Microstructure was characterized using a QUANTA 200 SEM. Chemical composition was measured by EDAX energy dispersive X-ray(EDX) spectroscopy. An HXS-1000 microhardness tester was used to determine the Vickers hardness of the

sintered structure at a load of 0.98 N and an indentation time of 20 s.

3 Results and discussion

3.1 Phase analysis

Fig.3 shows the typical XRD patterns of the starting powder mixture and the laser sintered sample. The powder system mainly consists of a matrix metal Cu and a ceramic phase WC, while Co peaks are weak due to its relatively small content (Fig.3(a)). After laser sintering, the strong diffraction peaks of Cu (FCC structure) and WC (hexagonal structure) can be observed (Fig.3(b)). This indicates that laser sintering process does not lead to any compositional changes of the matrix phase and the reinforcing phase. Furthermore, Fig.3(b) reveals the presence of a metastable phase $CoC_{0.25}$. During laser sintering, the Cu powder tends to melt due to the relatively low melting point of 1 083 ℃, while the spreading of binder phase Co is also expected to occur after the temperature has reached 1 000 ℃ for fine grained WC-Co powder[13,14]. With the wetting of the molten Co and Cu, a portion of sub-micro WC tends to dissolve in the liquid[15]. HAGLUND et al[16] confirmed that in the molten Co, the diffusion coefficient of W(6.9×10^{-15} m^2/s at 1 200 ℃) is much smaller than the diffusion coefficient of C (4.43×10^{-11} m^2/s at 1 200 ℃). Thus, the C diffuses preferentially towards the Co. However, due to the highly non-equilibrium effects caused by the extremely short laser sintering time such as large degrees of undercooling and high solidification rate, carbon atoms have insufficient time to diffuse into the CoC_x lattice, which leads to the formation of the metastable solidifying phase.

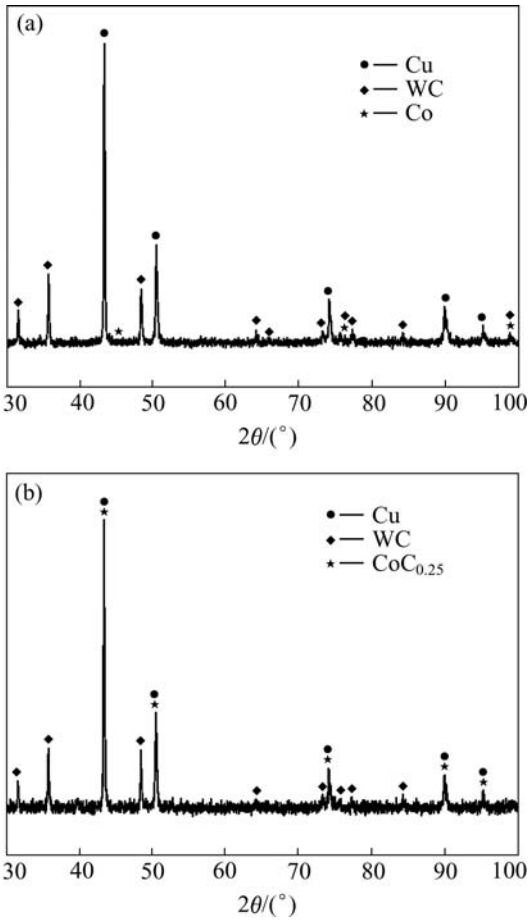

Fig.3 XRD patterns of starting powder system(a) and laser sintered sample(b)

3.2 Microstructure

Fig.4 shows the microstructure on the polished section of the laser sintered sample. It can be seen that no apparent pores are formed, showing a pretty dense structure. Fig.5 shows the characteristic microstructure of the etched sample at a higher magnification. It is clear that the sintered structure consists of the Cu matrix and the inserted WC particulates with the main composition of 53.02%W(mass fraction) and 39.17%C (measured by EDX at point *C*). In order to further investigate the distribution of various elements in the sintered structure, an EDX line-scan was performed from *A* to *B* (Fig.5), with the distributions of W, C, Cu, and Co shown in Fig.6. In the middle of the scan-line where the reinforcing particulates appear, the W content increases sharply and remains at high values (Fig.6(a)), while the C content also shows a slight increase (Fig.6(b)). In the exterior of the reinforcing particulates, the Cu content increases steeply (Fig.6(c)), indicating the sufficient coating of WC particulates by Cu matrix. Furthermore, the Co element exhibits a homogeneous distribution along the scan-line (Fig.6(d)). At an initial stage of laser sintering, the binder phase Co is expected to melt and spread at a relatively low sintering temperature since the sub-micro WC-Co composite powder with fine grains is used[13, 16]. With a further action of laser irradiation, the Cu matrix also melts to form liquid phase. Consequently, a molten pool containing both liquid

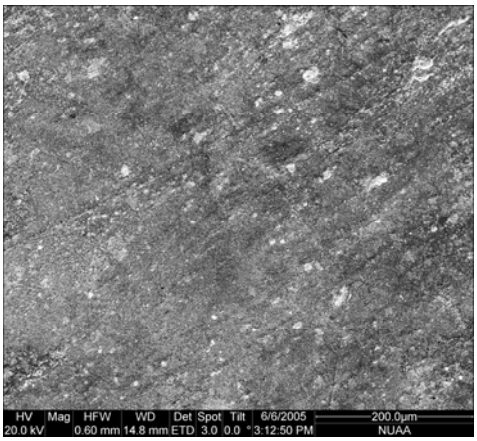

Fig.4 SEM image of microstructure on polished section of laser sintered sample

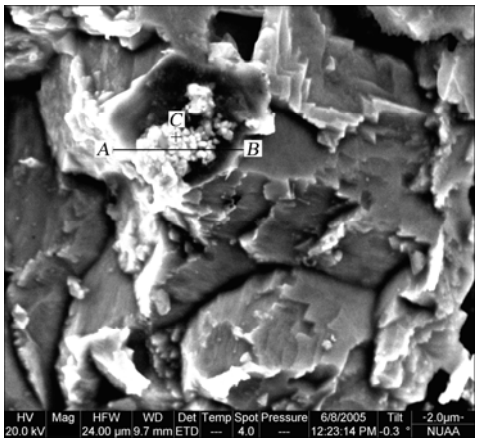

Fig.5 SEM image of etched microstructure of laser sintered sample

phase(Co and Cu) and solid phase(WC) is expected to be formed. Because a Gaussian laser beam is used, a large temperature gradient forms between the center and edge of the pool. The presence of the temperature gradient gives rise to a surface tension gradient and resultant Marangoni convection[11]. The formation of Marangoni convection induces capillary forces for liquid flow and particle rearrangement, thereby facilitating an efficient densification of solid particles with the wetting liquid (Fig.4). Due to the relatively high solubility of Co in Cu as well as the uniform dispersing state of the molten Co formed at the initial stage of laser sintering, a homogeneous distribution of the Co element in the Cu matrix can be obtained. As to WC particulates, the rapid rearrangement of solid particles may occur under the influence of capillary forces exerted on them by the wetting liquid. However, due to the negligible solubility of WC in Cu, WC particulates may be pushed away from Cu phase and segregate along the solidified Cu, resulting in the formation of such WC-cored and Cu-coated structures (Figs.5 and 6).

The WC reinforcing particulates in the sintered structure typically have three kinds of morphologies, as exhibited respectively in Fig.7. Fig.7(a) shows the first morphology of the reinforcing particulates, which has an irregular polygonal shape and a mean particle size of 0.6 μm. Compared with the original morphology of WC particulates (Fig.1), it is reasonable to consider that WC particulates are undissolved. Furthermore, significant aggregation of WC particulates occurs in this case. During laser sintering, the duration of the laser beam on any irradiating region is extremely short, typically less than 4 ms[2]. Therefore, the significant melting and subsequent smoothing of the larger WC particulates may not occur due to the relatively higher melting point. This suppresses the sufficient rearrangement of particles in the molten liquid, thereby resulting in particulate aggregation.

The second kind of the reinforcing particulates is shown in Fig.7(b). Some smooth and round particulates are visible, which indicates the melting of the edges of

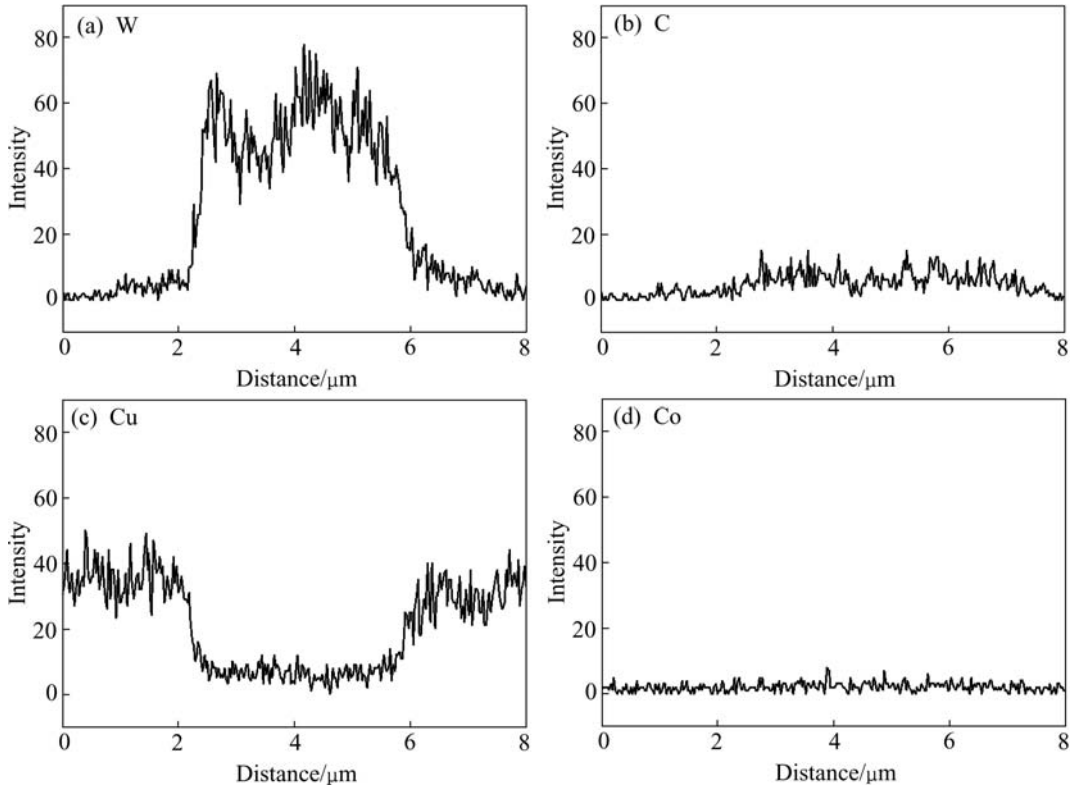

Fig.6 EDX patterns of distributions of W(a), C(b), Cu(c), and Co(d) along *AB* line in Fig.5

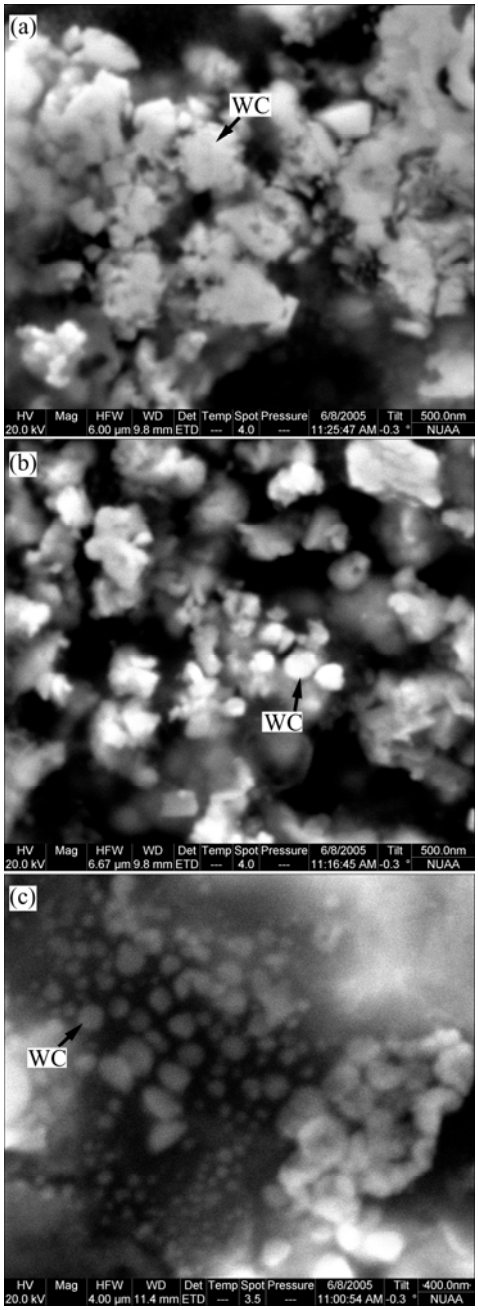

Fig.7 SEM images of morphologies of WC particulates in sintered structure: (a) Agglomerated and undissolved; (b) Incompletely separated and partially dissolved; (c) Separated and dissolved

WC particulates. Meanwhile, the dispersing homogeneity of WC particulates shows an improvement in this instance. In fact, these two kinds of WC particulates are essentially alike in their attributes, since neither of them dissolves completely. The difference of the two morphologies arises from the degree of dissolution and dispersion of WC particulates, which mainly depends on the powder characteristics (e.g. particle shape, particle size and its distribution) and the local temperature in the molten pool. Therefore, the arrangement ratio of WC particulates in liquid phase sintering process plays a key role in determining a sound sinterability.

The third kind of particulates, as shown in Fig.7(c), has a completely different morphology from the above two particulates. The mean particle size is refined to 100 nm, while ultra-fine particulates with the size of 40 nm are visible in some zones. Furthermore, a homogeneous dispersion of the reinforcing particulates in the matrix is obtained. In this case, the original WC particulates are expected to be completely dissolved in the molten pool. Due to the highly non-equilibrium nature of laser processing such as high degrees of supercooling and rapid solidification rate, the molten WC precipitates again in the form of refined and dispersed particles. Further analysis shows that the diversity of the morphologies of WC particulates may arise from the non-uniform size distribution of the original WC-Co powder, which may eventually results in the variation of sintering mechanism. The larger WC particles remain in undissolved or partially dissolved state, with the dominant mechanism being particle rearrangement; while the sintering mechanism changes into dissolution-precipitation for the smaller WC particles.

3.3 Microhardness

Fig.8 shows the profile of microhardness measured across the cross-section of the laser sintered sample. The average value, $HV_{0.1}$268.5, is much higher than that of common casting or powder metallurgy copper and copper alloys (HV120-160)[19]. This is mainly ascribed to WC particulate reinforcement. Combined with XRD and SEM results, it is reasonable to confirm that WC particulate reinforced Cu matrix composite materials can be successfully fabricated by SLS process, in spite of the various morphologies of WC particulates. However, the microhardness fluctuates considerably (Fig.8). This may be attributed to the inhomogeneous distribution of WC reinforcing particulates in Cu matrix (Figs.7(a) and (b)). The chief causes are as follows: firstly, the original

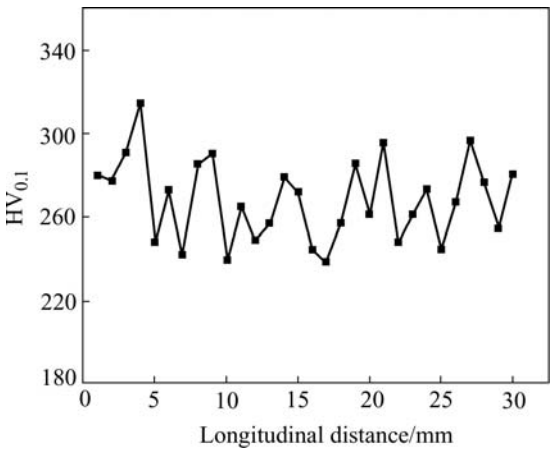

Fig.8 Variation of microhardness across cross-section of laser sintered sample

sub-micro WC-Co composite powder is still agglomerated after ball milling; secondly, the molten pool experiences high cooling rate during laser sintering, which suppresses the sufficient rearrangement of WC particulates.

4 Conclusions

1) Through the liquid phase sintering mechanism, the WC-10%Co particulate reinforced Cu matrix composite material is successfully fabricated by selective laser sintering.

2) The non-equilibrium effect induced by laser melting such as high degrees of undercooling and high solidification rate results in the formation of a metastable phase $CoC_{0.25}$.

3) The WC reinforcing particulates typically have three kinds of morphologies, that is, agglomerated and undissolved, incompletely separated and partially dissolved, separated and dissolved. Particle rearrangement acts as the dominant sintering mechanism for the larger WC, while dissolution-precipitation prevails for the smaller WC particles.

4) The average microhardness of the laser sintered sample is $HV_{0.1}$268.5, but the hardness varies considerably. This is attributed to the segregation of WC particulates and the high solidification rate experienced by the molten pool.

Acknowledgements

The authors would like to thank Prof. WANG Yang, Dr. YANG Jia-lin, and Dr. SHEN Xian-feng for their helps in the preparation of the laser sintered specimens. The helps of Mr. HU Xiao-yun and Dr. LIU Jin-song in the SEM and XRD investigations are also appreciated.

References

[1] ZHU H H, FUH J Y H, LU L. Microstructural evolution in direct laser sintering of Cu-based metal powder [J]. Rapid Prototyping Journal, 2005, 11(2): 74−81.

[2] SIMCHI A, ASGHARZADEH H. Densification and microstructural evaluation during laser sintering of M2 high speed steel powder[J]. Materials Science and Technology, 2004, 20(11): 1462−1468.

[3] BAI Pei-kang, CHENG Jun, LIU Bin. Selective laser sintering of polymer-coated Al_2O_3/ZrO_2/TiC ceramic powder[J]. Trans Nonferrous Met Soc China, 2005, 15(2): 261−265.

[4] TOLOCHKO N, MOZZHAROV S, LAOUI T, FROYEN L. Selective laser sintering of single- and two-component metal powders[J]. Rapid Prototyping Journal, 2003, 9(2): 68−78.

[5] KRUTH J P, FROYEN L, VAN VAERENBERGH J, MERCELIS P, ROMBOUTS M, LAUWERS B. Selective laser melting of iron-based powder[J]. Journal of Materials Processing Technology, 2004, 149(1-3): 616−622.

[6] TANG Y, LOH H T, WONG Y S, FUH J Y H, LU L, WANG X. Direct laser sintering of a copper-based alloy for creating three-dimensional metal parts[J]. Journal of Materials Processing Technology, 2003, 140(1−3): 368− 372.

[7] KHAING M W, FUH J Y H, LU L. Direct metal laser sintering for rapid tooling: processing and characterisation of EOS parts[J]. Journal of Materials Processing Technology, 2001, 113(1−3): 269−272.

[8] DAS S, BEAMAN J J, WOHLERT M, BOURELL D L. Direct laser freeform fabrication of high performance metal components[J]. Rapid Prototyping Journal, 1998, 4(3): 112−117.

[9] SIMCHI A, PETZOLDT F, POHL H. On the development of direct metal laser sintering for rapid tooling[J]. Journal of Materials Processing Technology, 2003, 141(3): 319−328.

[10] ZHU H H, LU L, FUH J Y H. Development and characterisation of direct laser sintering Cu-based metal powder[J]. Journal of Materials Processing Technology, 2003, 140(1-3): 314−317.

[11] SIMCHI A, POHL H. Effects of laser sintering processing parameters on the microstructure and densification of iron powder[J]. Materials Science and Engineering A, 2003, 359(1−2): 119−128.

[12] XU Cheng-ting, SHEN Yi-fu, GU Dong-dong, YANG Jia-lin, WANG Yang. Studies on sintering mechanism of Ni-CuSn-CuP mixed powder in selective laser sintering process[J]. Rare Metal Materials and Engineering, 2005, 34(Suppl.2): 341−344. (in Chinese)

[13] BREVAL E, CHENG J P, AGRAWAL D K, GIGL P, DENNIS A, ROY R, PAPWORTH A J. Comparison between microwave and conventional sintering of WC/Co composites[J]. Materials Science and Engineering A, 2005, 391(1−2): 285−295.

[14] PETERSSON A, ÅGREN J. Sintering shrinkage of WC-Co materials with bimodal grain size distributions[J]. Acta Materialia, 2005, 53(6): 1665−1671.

[15] GILLIA O, BOUVARD D. Phenomenological analysis of densification kinetics during sintering: application to WC-Co mixture[J]. Materials Science and Engineering A, 2000, 279(1−2): 185−191.

[16] HAGLUND S, ÅGREN J. W content in Co binder during sintering of WC-Co[J]. Acta Materialia, 1998, 46(8): 2801−2807.

[17] MAEDA K, CHILDS T H C. Laser sintering (SLS) of hard metal powders for abrasion resistant coatings[J]. Journal of Materials Processing Technology, 2004, 149(1-3): 609−615.

[18] YANG Ming-chuan. Preparation of WC-Co Based Nanocomposite Powders and Alloy[D]. Shenyang: Institute of Metal Research, Chinese Academy of Sciences, 2004. 25−32.(in Chinese)

[19] WANG Ai-hua, XIE Chang-sheng, HUANG Wei, XU Chun-yan. The laser-cladding of Al bronze on an Al-Si alloy[J]. Rare Metal Materials and Engineering, 1997, 26(6): 41−46. (in Chinese)

(Edited by YUAN Sai-qian)